

Crystal Structures of Cytochrome P-450_{CAM} Complexed with Camphane, Thiocamphor, and Adamantane: Factors Controlling P-450 Substrate Hydroxylation^{†,‡}

Reetta Raag[§] and Thomas L. Poulos*

Center for Advanced Research in Biotechnology of the Maryland Biotechnology Institute, University of Maryland at Shady Grove, 9600 Gudelsky Drive, Rockville, Maryland 20850, and the Department of Chemistry and Biochemistry, University of Maryland, College Park, Maryland 20742-5115

Received September 26, 1990; Revised Manuscript Received December 4, 1990

ABSTRACT: X-ray crystal structures have been determined for complexes of cytochrome P-450_{CAM} with the substrates camphane, adamantane, and thiocamphor. Unlike the natural substrate camphor, which hydrogen bonds to Tyr96 and is metabolized to a single product, camphane, adamantane and thiocamphor do not hydrogen bond to the enzyme and all are hydroxylated at multiple positions. Evidently the lack of a substrate-enzyme hydrogen bond allows substrates greater mobility in the active site, explaining this lower regioselectivity of metabolism as well as the inability of these substrates to displace the distal ligand to the heme iron. Tyr96 is a ligand, via its carbonyl oxygen atom, to a cation that is thought to stabilize the camphor-P-450_{CAM} complex [Poulos, T. L., Finzel, B. C., & Howard, A. J. (1987) *J. Mol. Biol.* 195, 687-700]. The occupancy and temperature factor of the cationic site are lower and higher, respectively, in the presence of the non-hydrogen-bonding substrates investigated here than in the presence of camphor, underscoring the relationship between cation and substrate binding. Thiocamphor gave the most unexpected orientation in the active site of any of the substrates we have investigated to date. The orientation of thiocamphor is quite different from that of camphor. That is, carbons 5 and 6, at which thiocamphor is primarily hydroxylated [Atkins, W. M., & Sligar, S. G. (1988) *J. Biol. Chem.* 263, 18842-18849], are positioned near Tyr96 rather than near the heme iron. Therefore, the crystallographically observed thiocamphor-P-450_{CAM} structure may correspond to a nonproductive complex. Disordered solvent has been identified in the active site in the presence of uncoupling substrates that channel reducing equivalents away from substrate hydroxylation toward hydrogen peroxide and/or "excess" water production. A buried solvent molecule has also been identified, which may promote uncoupling by moving from an internal location to the active site in the presence of highly mobile substrates.

The cytochrome P-450 superfamily of enzymes catalyzes many different types of oxidative reactions involved in steroid hormone biosynthesis, fatty acid metabolism, and detoxification of foreign compounds (Nebert et al., 1981; Nebert & Gonzalez, 1987; Anders, 1985). Xenobiotic-metabolizing P-450s generally oxidize substrates to more soluble forms, facilitating their excretion. Occasionally these products linger in the cytoplasm as "activated" electrophilic compounds, many of which are mutagens and/or carcinogens (Heidelberger, 1975; Sato & Omura, 1978; Anders, 1985; Ortiz de Montellano, 1986; Wolf, 1986). Due to the broad substrate specificity of this superfamily, and its ability to catalyze multiple types of reactions, there is much interest in structure-function relationships of P-450s. Ultimate goals include designing compounds to selectively inhibit individual P-450s and engineering novel P-450s to facilitate detoxification of specific environmental contaminants.

The best characterized P-450, and the only one for which a crystal structure is known, is the bacterial camphor hydroxylase P-450_{CAM} (Gunsalus et al., 1974; Debrunner et al.,

1978; Gunsalus & Sligar, 1978; Ullrich, 1979; Wagner & Gunsalus, 1982; Poulos et al., 1985, 1987). The reaction cycle of cytochrome P-450_{CAM} is shown in Figure 1. Besides hydroxylating camphor, P-450_{CAM} will also hydroxylate various other compounds. We have determined the X-ray crystal structures of ferric cytochrome P-450_{CAM} complexed with different substrates and inhibitors, as well as in the ferrous carbon monoxide and camphor bound form (Raag & Poulos, 1989a,b, 1990; Raag et al., 1990). These structures, together with data on substrate-dependent parameters and site-directed mutagenesis of P-450s (White et al., 1984; Fisher & Sligar, 1985; Atkins & Sligar, 1988a,b), have enabled us to better understand factors that influence regioselectivity and efficiency of P-450 reactions. Here we extend these studies to include three additional substrates. All substrate-P-450_{CAM} coordinates have been submitted to the Brookhaven Protein Data Bank (Bernstein et al., 1977).

MATERIALS AND METHODS

Thiocamphor synthesis was according to Scheeren et al. (1973) with the exception that P₂S₅ (FLUKA, Ronkonkoma, NY) was used in place of P₄S₁₀. Samples were analyzed (Galbraith Laboratories, Knoxville, TN) for C, H, O, and S to confirm that the correct compound had been prepared. P-450_{CAM} was crystallized according to our earlier procedure (Poulos et al., 1982). To prepare the various substrate-P-450_{CAM} complexes, crystals were soaked in a mother liquor

[†]Supported in part by NIH Grant GM 33688.

[‡]Crystallographic coordinates have been submitted to the Brookhaven Protein Data Bank under the following file names: 4CPP, cytochrome P-450_{CAM}-adamantane; 6CPP, cytochrome P-450_{CAM}-camphane; 8CPP, cytochrome P-450_{CAM}-thiocamphor.

*Correspondence should be addressed to T.L.P. at CARB.

[§]University of Maryland.

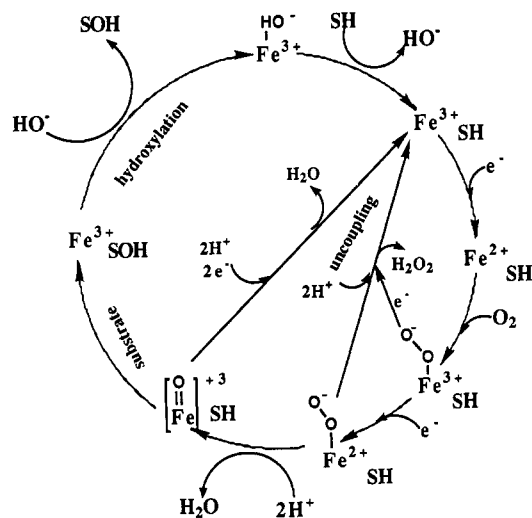


FIGURE 1: P-450 reaction cycle [modified from Atkins and Sligar (1988a)]. SH and SOH represent substrate and oxidized substrate, respectively. "Uncoupling" reactions compete with substrate hydroxylation. "Efficiency" refers to the percentage of reducing equivalents utilized toward substrate oxidation, as opposed to hydrogen peroxide/"excess" water production.

Table I: Summary of Substrate-P-450 Data Collection

substrate	camphane	adamantane	thiocamphor
max resolutn	1.91 Å	2.11 Å	2.09 Å
total observatns	108 560	144 737	133 336
R_{sym}^a	0.067	0.079	0.058
% data collected to	3.47 Å, 100%	3.82 Å, 100%	3.79 Å, 100%
	2.76 Å, 100%	3.04 Å, 100%	3.01 Å, 100%
	2.41 Å, 100%	2.65 Å, 100%	2.63 Å, 100%
	2.19 Å, 100%	2.41 Å, 100%	2.39 Å, 100%
	2.03 Å, 72%	2.24 Å, 100%	2.22 Å, 100%
	1.91 Å, 45%	2.11 Å, 73%	2.09 Å, 54%
$I/\sigma(I)$	2.19 Å, 1.91	2.41 Å, 2.50	2.13 Å, 2.15
	2.03 Å, 1.08	2.24 Å, 1.46	2.11 Å, 2.13
	1.91 Å, 0.55	2.11 Å, 0.72	2.09 Å, 0.24

^a $R_{sym} = \sum |I_i - \langle I_i \rangle| / \sum I_i$ where I_i = intensity of the i th observation and $\langle I_i \rangle$ = mean intensity.

consisting of 40% saturated ammonium sulfate, 0.05 M potassium phosphate, and 0.25 M KCl at pH 7.0, with saturating amounts of camphane, adamantane, or thiocamphor. Soak times were about three to four days. X-ray diffraction data were collected from single crystals of the various substrate-P-450_{CAM} complexes by using a Siemens area detector/Rigaku rotating anode and processed by using the XENGEN program package (Howard et al., 1987) on a Digital Equipment Corporation Microvax II. Data collection statistics are presented in Table I.

Substrates were initially sketched by using the Chemnote two-dimensional molecular construction facility in the molecular modeling package QUANTA (Polygen Corp., Waltham, MA), installed on a Silicon Graphics IRIS workstation. Following two-dimensional model building, substrate coordinates were energy minimized, again through QUANTA, using CHARMM steepest descents and Newton-Raphson energy minimization procedures. Substrate van der Waals volumes were calculated with QUANTA as well. Thiocamphor was modeled by substituting sulfur for oxygen in camphor, with the sulfur-carbon bond length maintained at the corresponding value for the oxygen-carbon bond. Such a model for thiocamphor should be adequate since the bond orders of C=S and C=O bonds are similar (Demarco et al., 1969).

Crystallographic refinement was carried out by using the

Table II: Summary of Substrate-P-450 Crystallographic Refinement

substrate	camphane	adamantane	thiocamphor
resolutn range (Å)	10.0-1.9	10.0-2.1	10.0-2.1
reflectns measured	27 786	20 548	22 650
reflectns used ^a	20 585	15 174	19 565
R factor ^b	0.190	0.184	0.175
rms deviation of bond dist (Å)	0.020	0.019	0.020
bond angles (Å)	0.032	0.033	0.033
dihedral angles (Å)	0.036	0.037	0.036

^a Reflections with $I > 2\sigma(I)$; I = intensity. ^b $R = \sum |F_o - F_c| / \sum F_o$.

(Hendrickson & Konnert, 1980) and is summarized in Table II. Initial $F_o - F_c$ and $2F_o - F_c$ difference Fourier maps were based on structure factor calculations using coordinates from the 1.7-Å refined camphor-P-450_{CAM} structure (Poulos et al., 1987) and diffraction data obtained from the substrate-P-450_{CAM} complexes. Camphor coordinates were not included in the initial structure factor calculations. $F_o - F_c$ maps were contoured at $\pm 3\sigma$ and $2F_o - F_c$ maps were contoured at $+0.5$ and $+1\sigma$ (σ is the standard deviation calculated over an entire asymmetric unit of the electron density map). Substrates were positioned into the $F_o - F_c$ maps and refined together with the protein, with substrate temperature factors initially starting at 19-20 Å², or near the mean temperature factor for all protein and heme atoms in the camphor-P-450_{CAM} structure. Structures were judged to have refined sufficiently once $F_o - F_c$ maps showed little or no interpretable density when contoured at 3σ . Initial $F_o - F_c$ and final $2F_o - F_c$ maps are shown in Figures 2 and 3. Refined models were subjected to additional refinement without bond, angle, or nonbonded contact distance restraints to better estimate active site distances. Comparison of both coordinate and temperature factor shifts was carried out as described elsewhere (Poulos & Howard, 1987).

RESULTS

Figures 2 and 3 show the initial $F_o - F_c$ and final $2F_o - F_c$ maps of the camphane-, adamantane-, and thiocamphor-P-450_{CAM} complexes. Modeling of camphane and adamantane bound to the enzyme was relatively straightforward. However, neither adamantane nor camphane is able to hydrogen bond to P-450_{CAM} and so we cannot be sure that these substrates do not occupy multiple orientations. Since models with single orientations for these substrates were successful in eliminating most of the difference electron density from the active site region, we take this as evidence that at least the major binding orientations of these substrates have been identified.

Camphane. Despite the similarity in structure and binding orientation between camphane and camphor, the atomic temperature factors of camphane refined to values (30 Å²) about twice those of camphor (16 Å²). This indicates that camphane is highly mobile when bound to P-450_{CAM}. One factor that could artificially raise temperature factors is an inaccurate model. We modeled the observed active site electron density with a single, fully occupied camphane molecule, but such a model would be inaccurate if the camphane occupancy in the crystal was incomplete. This is feasible since neither camphane nor adamantane was especially soluble in the crystallization mother liquor. However, since we were able to successfully model these substrates with full occupancy, the contribution

¹ Abbreviations: F_c , calculated structure factors; F_o , observed struc-

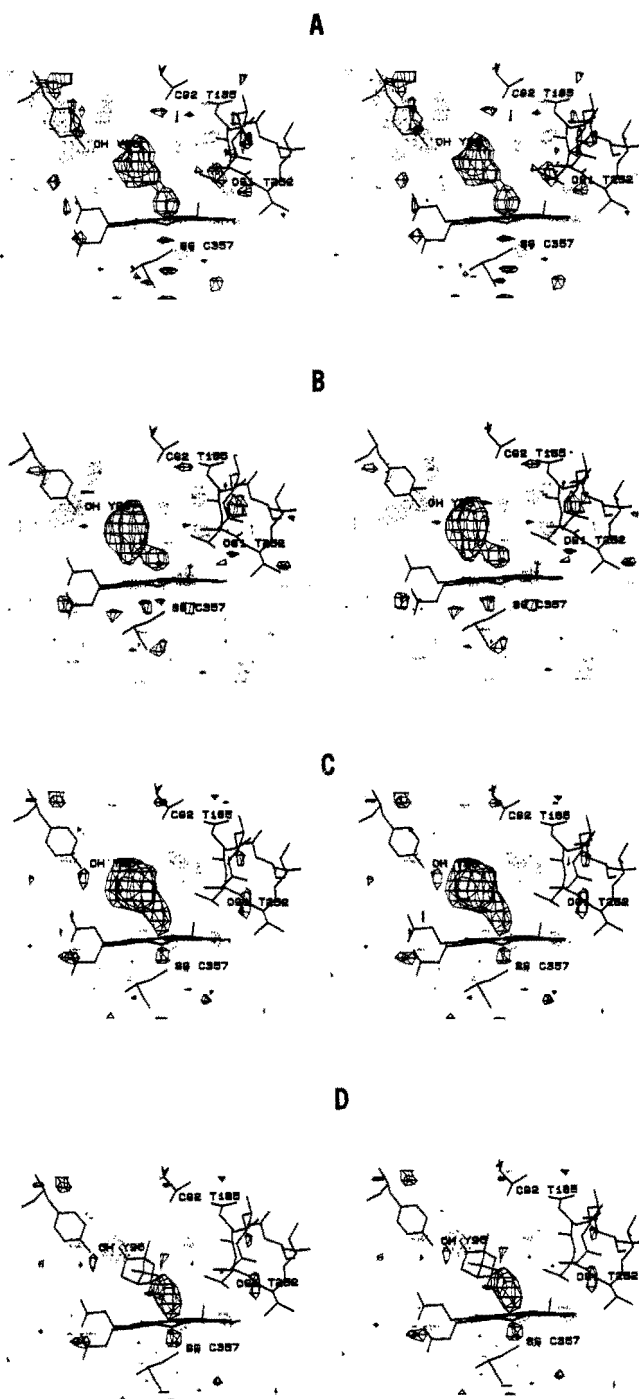


FIGURE 2: Initial $F_0 - F_c$ difference electron density maps for P-450_{CAM} complexed with camphane (A), adamantane (B), and thiocamphor (C, D). Maps were calculated with diffraction amplitudes from substrate-P-450_{CAM} complexes and phases from camphor-P-450_{CAM} coordinates (Poulos et al., 1987). Maps are contoured at $\pm 3\sigma$ with negative and positive density depicted as dotted and solid lines, respectively. Substrate coordinates were not included in phase calculations for maps A, B, and C, but camphor coordinates were included in the calculation of map D. Map D, with the camphor carbonyl oxygen in negative density and with positive density between the substrate and heme, indicates that thiocamphor binds "upside down" in the active site, compared with camphor. Note the electron density corresponding to the distal ligand to iron in all maps.

from the substrate-free structure is probably minimal (less than 20%). The presence of minor, unmodeled, binding orientations due to the lack of an enzyme-substrate hydrogen bond also could artificially raise substrate temperature factors.

With these caveats in mind, we still believe the high tem-

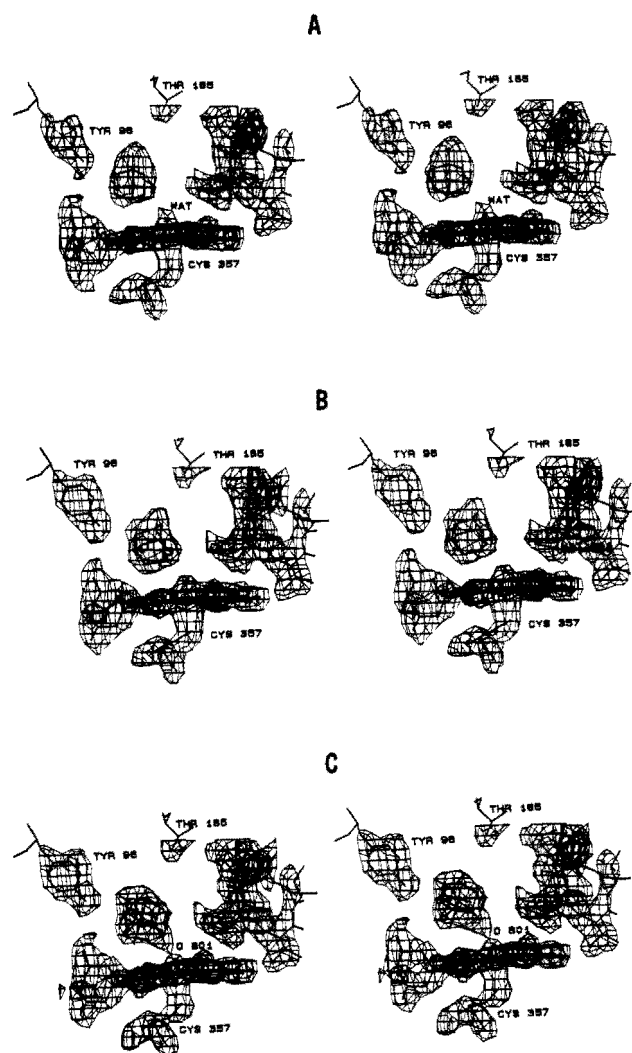


FIGURE 3: Final $2F_o - F_c$ electron density maps for P-450_{CAM} complexed with camphane (A), adamantane (B), and thiocamphor (C). Substrate and distal ligand coordinates were omitted from phase calculations for the maps shown. Note the electron density corresponding to the distal ligand to iron in all maps.

the temperature factors of Tyr96 side-chain atoms in the camphane-P-450_{CAM} structure are in the vicinity of 28 Å² and only about 13 Å² in the camphor-P-450_{CAM} complex, suggesting that the high camphane atomic temperature factors are real.

Adamantane. Temperature factors of Tyr96 side-chain atoms were about 19 Å² in adamantane-bound and 10 Å² in adamantane-bound P-450_{CAM} structures. These values are consistent with the lower average temperature factor of adamantane (24 Å²) than camphane and indicate that adamantane is less mobile than camphane when bound by P-450_{CAM}. We were concerned about this implication, considering that adamantane is highly symmetric and smaller than camphane and that neither substrate is able to hydrogen bond to the enzyme. Therefore we performed several refinement experiments.

Using the refined coordinates for adamantane-P-450_{CAM}, with an *R* factor of 18.1%, we repositioned adamantane in the substrate electron density in two different ways: (1) by approximately switching the locations of secondary and tertiary carbons and (2) by approximately switching the locations of atoms and bonds. Both of these repositionings resulted in a somewhat poorer fit of the substrate to the electron density.

perature factors of all atoms and occupancies of solvent atoms were refined alternately. In both experiments, the average temperature factor of adamantane increased by about 2.5 Å² (to 26.1 and 25.9 Å², respectively). Ten control refinement cycles increased the temperature factor of the best-fit adamantane model by approximately 1.0 Å² to 24.7 Å². In all three cases, the *R* factor dropped only 0.1% to 18.0%. However, electron density maps calculated with both sets of repositioned coordinates contained substantial amounts of $\pm 3\sigma$ $F_o - F_c$ difference electron density, indicating that the substrate was incorrectly positioned.

Our next two experiments involved fixing the temperature factors of all adamantane atoms arbitrarily at 16.0 and 32.0 Å² and calculating electron density maps to determine if there would be any observable effects. No differences were found either in *R* factor or in electron density maps when refined adamantane temperature factors (23.6 Å² average) or arbitrary ones of 32.0 Å² were used. However, when adamantane atomic temperature factors were set to 16.0 Å², although the *R* factor remained at 18.0%, positive 3σ difference electron density appeared around the substrate in the $F_o - F_c$ map, suggesting that the new temperature factors were incorrect.

In the final adamantane refinement experiment, the adamantane model considered best fit to the electron density was again used but all substrate atomic temperature factors were started at 32.0 Å². After 10 refinement cycles, the average atomic temperature factor for adamantane rose insignificantly to 32.1 Å², rather than dropping toward the previously determined value of 23.6 Å². Once again, the *R* factor remained at 18.0% and difference electron density maps showed no indication that substrate temperature factors might be incorrect. On the basis of these refinement experiments, we cannot give a definitive value for the adamantane temperature factor, but we regard it as being somewhere in the neighborhood of 25–32 Å².

Thiocamphor. In the initial thiocamphor $F_o - F_c$ map, which was based on camphor-P-450_{CAM} coordinates without camphor included, the substrate appeared to be binding “upside down” with respect to camphor (Figure 2C). Thus a second $F_o - F_c$ map was calculated, again based on the camphor-P-450_{CAM} coordinates, but this time including camphor coordinates, in their original orientation, in the phase calculation. When this map was contoured at $\pm 3\sigma$, the camphor carbonyl oxygen was found to occupy a region of negative difference electron density and a large region of positive difference electron density remained between the substrate and heme (Figure 2D). Although it seemed apparent that thiocamphor and camphor do not bind to P-450_{CAM} in the same orientation, another map was calculated, based on coordinates in which thiocamphor occupied the same orientation as camphor and in which an additional water molecule was included to occupy the positive density near the distal heme ligation site. As expected, the thiocamphor sulfur atom was surrounded by negative density and the water ligand was insufficient to account fully for the positive density between thiocamphor and the heme. Next, the distal water ligand was removed and thiocamphor was rotated (by approximately 180° in the plane of Figures 2 and 3) so that the thiocarbonyl was no longer directed toward Tyr96 but was directed toward the heme iron. Maps based on this model contained much less difference electron density but some positive difference density still remained between the sulfur and the heme iron. After including the distal ligand again, with thiocamphor in the new “upside down” orientation (Figure 4A), only a small amount of positive

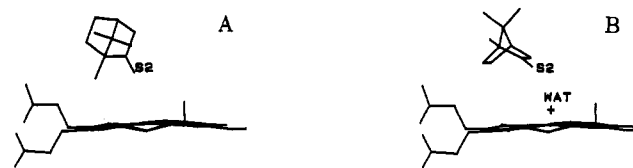


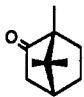
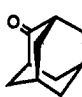

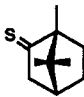
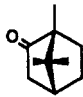
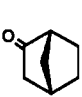

FIGURE 4: Comparison of the two different binding orientations determined crystallographically for thiocamphor. The presence of the distal ligand is only compatible sterically with the minor (30%) orientation shown on the right.

sulfur atom: positive between the substrate and porphyrin ring; negative between the substrate and distal helix. Since a rotation of the sulfur to better accommodate this residual density resulted in a much deteriorated fit of the thiocamphor methyl groups to the electron density, we attempted to fit thiocamphor to the density in yet a third orientation. This orientation again had the sulfur directed toward the heme, but now the six-membered ring of the substrate was essentially parallel to the porphyrin plane (Figure 4B), rather than perpendicular as it had been previously (and as it is when camphor binds). The new $F_o - F_c$ map based on this thiocamphor orientation had considerable difference electron density, indicating that this was not the major binding orientation of thiocamphor.

Finally, we were best able to minimize the difference electron density by including thiocamphor in both orientations (Figure 4), neither corresponding to that of camphor. The occupancy of the first orientation was estimated and fixed at 70%. In this position the sulfur atom approaches to within 2.35 Å of the distal ligand and most likely displaces it. The occupancy of the second orientation was fixed at 30%, and in this position the sulfur atom is 3.80 Å from the distal ligand. Curiously enough, when the occupancy of the distal ligand was fixed at 0.30 (to correspond with the second thiocamphor orientation) and only its temperature factor allowed to refine, although the temperature factor dropped to quite a low value (10 Å²), positive difference density still remained around this ligand in $F_o - F_c$ maps. Nor did subsequent release of the fixed occupancy of the distal ligand, during refinement, remove the difference density, despite the fact that the occupancy climbed to 0.51 (after 20 refinement cycles; the temperature factor also dropped to 8.3 Å² during this time). These results suggest that occupancies and temperature factors are unable to recover, in a reasonable number of refinement cycles, from initial poor estimates of these values. They also confirm that though highly correlated, occupancies and temperature factors are not entirely interchangeable as modeling parameters.

We were only able to eliminate the difference electron density from around the distal ligand by including it initially with full occupancy and a temperature factor of 20.0 Å², near the mean temperature factor for all protein and heme atoms, and allowing both occupancy and temperature factor of this ligand to refine. In the final model, the distal ligand has a temperature factor of 19.6 Å² and an occupancy of 0.90 and $F_o - F_c$ maps calculated with these coordinates show no residual difference density around the sixth ligation position. The temperature factor of thiocamphor itself refined to about 23.5 Å², or about 50% higher than that of camphor bound in the active site. This higher mobility for thiocamphor, a larger substrate than camphor, suggests that thiocamphor may occupy additional minor orientations, possibly the one corresponding to camphor bound to the enzyme. Minor thiocamphor orientations which we have not modeled could potentially account also for the discrepancy between the occupancies of the distal ligand and of thiocamphor orientation 2

Table III: Various Substrate-Dependent Parameters^g

							
	camphor	adamantanone	adamantane	thiocamphor	camphor/Y96F	norcamphor	camphane
molec vol	315 Å ³	300 Å ³	293 Å ³	322 Å ³	315 Å ³	236 Å ³	309 Å ³
hydrogen bond to Y96	yes ^a	yes ^b	no	no	no	yes ^b	no
no. of iron ligands	5 ^a	5 ^b	6	6		6 ^b	6
redox pot. Fe ³⁺ /Fe ²⁺	-170 mV ^c	-175 mV ^c				-206 mV ^c	
high-spin %	94-97% ^{c-e}	96-98% ^{c,d}	99% ^d	65% ^e	59% ^e	46% ^c	46% ^e
regiospecific of substr hydroxylatn	5-exo (100%) ^{d,f}	5 (100%) ^d	1 (100%) ^d	5-exo (64%) ^e 6-exo (34%) 3-exo (2%)	5-exo (92%) ^{e,f} 4 (1%) 6-exo (2-4%) 3-exo (0-4%) 9 (<1%)	5-exo (45%) ^f 6-exo (47%) 3-exo (8%)	5-exo (90%) ^e 6-exo (10%)
substr temp factor (Fe ³⁺)	16.2 Å ^{2a}	16.5 Å ^{2b}	24.7 Å ²	23.5 Å ²		33.5 Å ^{2b}	30.1 Å ²
substr hydrophilic groups	yes	yes	no	yes	yes	yes	no
hydroxylatn "efficiency"	100% ^{e,f}			98% ^e	100% ^e	12% ^f	8% ^e
L6-substr dist	NA	NA	2.63 Å	2.35 Å (70%) 3.35 Å (30%)		3.0 Å ^b	2.88 Å
L6-iron dist	NA	NA	1.95 Å	1.35 Å		1.73 Å ^b	1.67 Å
L6 occupancy	NA	NA	1.00	0.90		0.97 ^b	1.00
L6 temp factor	NA	NA	14.3 Å ²	19.6 Å ²		3.8 Å ^{2b}	7.7 Å ²
cation occupancy	1.00 ^a	1.00 ^b	0.89	0.91		1.00 ^b	0.72
cation temp factor	12.1 Å ^{2a}	10.0 Å ^{2b}	15.5 Å ²	14.2 Å ²		7.9 Å ^{2b}	21.7 Å ²

^a Poulos et al. (1985, 1987). ^b Raag and Poulos (1989a). ^c Fisher and Sligar (1985). ^d White et al. (1984). ^e Atkins and Sligar (1988b). ^f Atkins and Sligar (1989). ^g Carbon numbering for each substrate begins with C-1 at the top of the six-membered ring which is in the plane of the table. Numbering proceeds counterclockwise such that the carbonyl carbon is C-2 and C-5 is in the lower right-hand portion of the ring. Note that C-5 is a secondary carbon in some substances and a tertiary carbon in others.

the distal ligand is located between the heme iron and the substrate sulfur atom. These two neighbors could conceivably interact via the distal ligand and increase electron density at this location, which could be reflected in an anomalously high ligand occupancy.

Although initial occupancy estimates for the two thiocamphor orientations were successful in eliminating substrate-associated difference electron density, we decided to explore other occupancy combinations because of the discrepancy between the refined occupancy of the distal ligand (0.90) and the estimated occupancy of the thiocamphor orientation (0.30), which would be sterically compatible with the presence of the ligand. After calculating and examining maps based on occupancy combinations ranging from 0.30/0.70 to 0.80/0.20 in increments of 0.10, we concluded that the relative occupancies of thiocamphor orientations 1 and 2 (parts A and B of Figure 4, respectively) are probably around 65% and 35%, respectively, with an error of roughly 10%.

DISCUSSION

Substrate Hydroxylation Profiles

Camphane. Although camphane is incapable of hydrogen bonding with Tyr96, its similarity to camphor in overall shape and size causes it to be bound in a nearly identical position in the P-450_{CAM} active site. The methyl groups of camphane and camphor interact with the same active site features. As with camphor, the 5-carbon atom of camphane is the nearest to the heme iron atom, explaining the observed preference (90% of products) for 5-exo hydroxylation of this substrate (Atkins & Sligar, 1988b). That 10% of the products are 6-exo hydroxylated (Atkins & Sligar, 1988b) can be attributed to the enhanced mobility of camphane in the P-450_{CAM} active site (Table III).

Hydroxylation profiles and crystallographic data on norcamphor- and camphane-P-450_{CAM} complexes, in comparison with camphor complexes, demonstrate that two features, a

Waals interactions, are both necessary to lower the mobility of a substrate. Low substrate mobility, as revealed by crystallographic temperature factors, appears to be critical for high regiospecificity of substrate metabolism (Table III).

Adamantane. Adamantane is the only substrate we have investigated, in this study, that is metabolized to a single product despite having a relatively high active site mobility. The single product can be attributed to the existence of only two types of unique carbon atoms in adamantane, together with the greater reactivity of tertiary versus secondary carbons (White et al., 1984).

Thiocamphor. Thiocamphor binds to P-450_{CAM} in two orientations, both of which are different from that preferred by camphor and both of which have sulfur as the substrate atom nearest to iron. A priori, the proximity of the sulfur atom to the heme suggests that the thiocamphor hydroxylation mechanism might involve an initial single electron transfer from sulfur to heme instead of, or in competition with, initial hydrogen abstraction, as is thought to occur with camphor (Ortiz de Montellano, 1986). However, the major products of thiocamphor metabolism are 5- and 6-exo hydroxylated, and these substrate atoms are among the farthest substrate atoms from the active oxygen location in our thiocamphor-P-450_{CAM} model. Modeling of thiocamphor in the orientation preferred by camphor (with full occupancy) resulted in difference electron density maps strongly suggesting that such a model was incorrect. Nevertheless, the products of thiocamphor hydroxylation imply that this substrate is only metabolized when it adopts a camphor-like orientation in the active site. These data lead us to conclude that the conformers seen in the crystal structure are nonproductive and that the camphor-like conformer is fractionally occupied and crystallographically unobservable. Although thiocamphor appears to make a snug van der Waals fit with P-450_{CAM}, it may be possible for it to occasionally rotate within the active site to yield a camphor-like complex, as suggested by molecular dy-

Explore Litigation Insights

Docket Alarm provides insights to develop a more informed litigation strategy and the peace of mind of knowing you're on top of things.

Real-Time Litigation Alerts



Keep your litigation team up-to-date with **real-time alerts** and advanced team management tools built for the enterprise, all while greatly reducing PACER spend.

Our comprehensive service means we can handle Federal, State, and Administrative courts across the country.

Advanced Docket Research



With over 230 million records, Docket Alarm's cloud-native docket research platform finds what other services can't. Coverage includes Federal, State, plus PTAB, TTAB, ITC and NLRB decisions, all in one place.

Identify arguments that have been successful in the past with full text, pinpoint searching. Link to case law cited within any court document via Fastcase.

Analytics At Your Fingertips



Learn what happened the last time a particular judge, opposing counsel or company faced cases similar to yours.

Advanced out-of-the-box PTAB and TTAB analytics are always at your fingertips.

API

Docket Alarm offers a powerful API (application programming interface) to developers that want to integrate case filings into their apps.

LAW FIRMS

Build custom dashboards for your attorneys and clients with live data direct from the court.

Automate many repetitive legal tasks like conflict checks, document management, and marketing.

FINANCIAL INSTITUTIONS

Litigation and bankruptcy checks for companies and debtors.

E-DISCOVERY AND LEGAL VENDORS

Sync your system to PACER to automate legal marketing.